

LA-UR-79-2846

**TITLE:** P-MATRIX ANALYSIS OF COMPOUND-ELEMENT REACTOR FUEL ELEMENT  
AFRL/ML/MS

**AUTHOR(S):** J. N. Hale and C. L. Gitter

**SUBMITTED TO:** To be presented at the International Conference of  
Nuclear Power Sections for Technology, Novosibirsk, USSR  
Oct. 22-26, 1979

W. L. Gitter

In accordance with the copyright notice on page 1, the  
author(s) conveys the Government's interest rights  
in the copyright and the Government and its authorized  
representatives have unrestricted right to reproduce or  
otherwise use said article under an copyright  
agreement with the publisher.

The Los Alamos Scientific Laboratory requests that the  
publisher identify this article as work performed under  
the auspices of the USDOE

  
**los alamos**  
scientific laboratory  
of the University of California  
LOS ALAMOS NEW MEXICO 87545

An Affirmative Action Equal Opportunity Employer

UNITED STATES  
ENERGY RESEARCH AND  
DEVELOPMENT ADMINISTRATION  
CONTRACT WITH THE DOE

## R-MATRIX ANALYSES OF LIGHT-ELEMENT REACTIONS FOR FUSION APPLICATIONS

G. E. Hale and T. C. Dudder  
Los Alamos Scientific Laboratory, University of California,  
Theoretical Division  
Los Alamos, New Mexico 87545, USA

ABSTRACT: The latest multi-channel R-matrix analyses, evaluated fusion cross sections, and applications.

In previous R-matrix analyses of reactions in light systems (primarily Li), interest has been focused on the fewest channels of interest in fusion applications. Results of analyses of the Li-7, Li-6, and Li-7-Li-7 systems are presented, with particular emphasis on the reaction of Li-7 with deuterium, tritium, and Li-7 in fusion reactions.

### INTRODUCTION

The fusion energy research program for the early 1970's has shown the need for theoretical calculations of reactions in light elements. These calculations are required to predict the energy requirements for the heating of the plasma, to determine the energy densities in the plasma, to remove and re-inject ions to heat the plasma, to remove and re-inject ions to heat the plasma, and to provide diagnostic information about plasma conditions.

For the early 1970's, different types of codes have been developed. These codes are based on the microscopic theory of nuclear reactions, and they are able to predict the energy requirements for the plasma.

For the early 1970's, different types of codes have been developed. These codes are based on the microscopic theory of nuclear reactions, and they are able to predict the energy requirements for the plasma.

The R-matrix theory has been described by several authors, but has been presented at several meetings, technical conferences.<sup>1-7</sup> In the case of charge-changing reactions of interest in fusion applications, the separation of short-ranged and long-ranged forces exist. In R-matrix theory, these effects and angular momentum effects, can be taken into account in a simple and natural way with nuclear effects, especially resonances. Also, since the R-matrix provides a particularly simple and unified parameterization of multi-channel scattering theory, one has the prospect of using the same parameters to describe several systems simultaneously, and in imposing a large amount of experimental information on the determination of the parameterized results. If unpaired states do not facilitate the predictions from the fit, in the following sections, we will describe the applications of multi-channel R-matrix theory to few-nucleon systems in the mass range A < 10 having charge-changing interactions of interest in fusion applications, without theory, however, with a brief, formal summary of R-matrix theory.

### Formal Summary of R-Matrix Theory

Imagine a nuclear scattering process in which A nucleons, total, are distributed between two bound

nuclei, i.e., protons, deuterium, and tritium, or deuterium, deuterium, tritium, and helium. The different nuclear channels of the nucleus are called the "channels" of the system, and the surface,  $r_c$ , defines the boundary of the channel. The other channels are called the "interior" surface,  $r_i$ . In the interior region of the nucleus, the interior surface or interior boundary is relatively small relative to configuration space for the nucleons. R-matrix theory relates the wavefunction in the large region outside the channel surface (which is most accessible to experiment), to that inside the channel surface in the form of boundary conditions for the wavefunction, the "channel equations".

Let us assume that the exterior region outside the channel surface is large enough so that the boundary conditions are well defined.

### Channel Equations

#### 1. The Channel Equations

##### a. The $\psi$ Function

One needs to define first the channel function,  $\psi$ , in exterior, exterior to the channel surface, and in the interior, interior to the channel surface, in terms of the channel boundary condition,  $r_c$ .

$$\psi = \psi(r)$$

can be made hermitian in the interior region by the appropriate choice of  $\psi$ , even though the hermitian  $\psi$  is not hermitian if  $\psi$  evolves to positive-energy channels at the surface. A choice for  $\psi$  that accomplishes this purpose is

$$\psi = \sum_c c(r) e^{i\theta_c(r)} \frac{\partial}{\partial r_c} \psi_c + \psi_c \quad (1)$$

with  $c(r) = \left( \frac{E}{E_{c,0}} \right)^{1/2} \frac{e^{-i\theta_c(r)}}{\sqrt{\psi_c}}$ , the "channel

surface function", defined in terms of the channel spin-angle eigenfunction of total angular momentum and parity  $\psi_c(r)$ , and  $E$ , the real, energy-independent boundary number specified at the channel surface,  $r_c = a_c$ , which generate the R-matrix theory of

Wigner and Eisenbud.<sup>8</sup>

Taking the projection of Eq. (1) on the channel surface, and inserting the forms (3) and (4), one obtains

$$(c' \cdot \vec{v}) = \sum_i (c'_i \cdot \vec{v}_i) (c_i - \frac{\partial}{\partial c_i} F_i - B_i) \quad (5)$$

Since  $c$  is known outside and on the channel surface (i.e., the "external" sector), as a superposition of Coulomb spherical waves,

$$c_i = \sum_j c_{ij} e^{i k_j r_{ij}} \quad (6)$$

the constants  $c_{ij}$  in the external wavefunctions can be expressed in terms of the elements of the R-matrix.

$$c_{ij} = \frac{1}{k_j} \int_{r_{ij}}^{\infty} r dr J_0(k_j r) R_{ij}(r) \quad (7)$$

It follows from the definition of  $R$ ,

$$R_{ij} = \frac{1}{2} \left[ \frac{1}{k_j} \int_{r_{ij}}^{\infty} r dr J_0(k_j r) \right] \left( \frac{1}{k_i} - \frac{1}{k_j} \right) \quad (8)$$

$$\text{where } k_i = \sqrt{\frac{2m_i E_i}{\hbar^2}} \quad (9)$$

is the Coulombic derivative of the scattering potential  $V$  at the energy  $E_i$  evaluated on the surface. The unitarity of the collision matrix  $U$  follows from the hermiticity of the R-matrix. The point of expressing the collision matrix, from which the results of any scattering measurement - cross section, polarization, etc. - can be obtained in terms of the R-matrix is that it is now a simple matter to identify the internal poles of the R-matrix elements in the internal region for the  $i$ -channel, and to use the properties of the R-matrix to obtain the location of the poles. In fact, if  $\lambda_i$  and  $\mu_i$  are the real and imaginary parts of the  $i$ -channel pole, we can usually call the " $\lambda_i$ " and " $\mu_i$ " respectively the "real" and "imaginary" parts of the pole, or simply the "real" and "imaginary" parts of the resonance.

Finally, if the poles are real enough, that is, if the coupling from the R-matrix results in a stable system, it is easy to make the R-matrix hermitian by shifting the eigenvalues of  $U$  to satisfy

$$U = U^* \quad (10)$$

for eigenvalues  $\lambda_i$  from a complete orthogonal set in the internal region. Assuming the  $\lambda_i$ 's are normalized, we have the expansion

$$G = \sum_i \frac{\lambda_i G_i}{E_i - F} \quad (11)$$

from which it follows immediately that

$$F_{c'c} = (c' \cdot G \cdot c) = \sum_i \frac{\lambda_i g_{ic}}{E_i - F} \quad (12)$$

where  $g_{ic} = (c'_i \cdot c)$  is the "reduced width amplitude". The simple pole term of the R-matrix expansion (10), characterized by the parameters  $\lambda_i$  and  $E_i$ , which depend on the channel radii  $r_c$  and boundary condition numbers  $B_c$ , can be identified with resonances of the compound A-nucleon system. However, not every pole term need be identified with a resonance in the conventional sense (i.e., one that shows a sufficiently narrow width  $T$  in the collision matrix to have a relatively long lifetime  $\tau = \hbar/T$ ). They can

also be identified with shorter-lived "direct" processes, like single-particle scattering, stripping, etc., since the R-matrix formalism is not specialized to a particular reaction mechanism. Contributions from these latter processes are especially important in applications to few-nucleon systems, as will be discussed in the following section.

### Applications

We will describe multi-channel R-matrices and code for the  $^3$ H,  $^4$ He,  $p-^3$ He, and  $p-^4$ He systems. We will compare some of the basic charged-particle elastic, reaction, and other calculations with various R-matrix techniques being used at Los Alamos. The first two and the last of these, which are the most general approach to these analyses, have been used to make use of all available data for all three systems. In each system, and to use the full multilevel, multichannel R-matrix expansion, it is approximated only by truncating the sum over levels. For a given choice of channel radii  $r_c$  and boundary condition numbers  $B_c$ , the R-matrix parameters  $\lambda_i$  and  $E_i$  are adjusted by an automated fitting procedure,  $\chi^2$ , to achieve a best fit in the least-squares sense to all the data included. The code also has the capability to treat the channel radii, as well as normalizations and energy shifts for the experimental data, as adjustable parameters.

### Two-Particle

We shall first concentrate on two-particle systems, with just the R-matrix parameters as adjustable, or such a way that in the  $T=0$  system, or in the  $p-^3$ He system, scattering amplitudes will be zero. This is not to say that the R-matrix technique is not useful for  $T \neq 0$ , and that the R-matrix technique is not appropriate for the analysis of nucleon-nucleon scattering, which is broader version of the internal Coulomb effects; this often says that the R-matrix and R-matrix + exchange theories (i.e., and in the case of the four-nucleon system, that the  $T=1$  part of the R-matrix which describes reactions in the  $^4$ He system is essentially the same as that which describes  $p-^3$ He scattering, which, in turn, is essentially the same as that which describes  $n-^3$ He scattering. Accounting for the differences in the  $T=1$  R-matrix parameters due to internal Coulomb effects by simply shifting the  $F_{ij}$ 's appears to work quite well. The  $T=1$  parameters for this system were actually determined by fitting most of the available  $p-^3$ He scattering data below 20 MeV. These parameters, energy-shifted to account for the decreased Coulomb repulsion energy in  $^4$ He, were used in a larger analysis of reactions among  $p-T$ ,  $n-^3$ He, and  $d-d$ , where only the energy shift and parameters for the  $T=0$  part of the R-matrix were adjusted to fit the data. In addition, isospin conservation relates the widths in the  $p-T$  and  $n-^3$ He channels for both  $T=0$  and  $T=1$  levels to reduce further the number of parameters.

A summary of the data included for each reaction in the  $^4$ He system analysis is given in Table I. The types of data to which the table refers generally

include cross sections (both differential and integrated) and polarizations for various spin orientations of the incoming and outgoing particles. The fits are, on the whole, good representations of the experimental measurements for all six reactions.

Table 1.  $^3\text{He}$  System Analysis

CHANNEL (INCOMING p-T)			
	n- $^3\text{He}$	d- $^3\text{He}$	
		$\Sigma \sigma_{\text{tot}}$	
Ref. #	Energy /MeV	Isospin State	No. Data Points
D. et al.	$E_p = 0.1$	1	137
Theus et al.	$E_p = 0.1$	5	721
n- $^3\text{He}$	$E_p = 0.1$	+	117
D. et al.	$E_p = 0.2$	+	697
n- $^3\text{He}$	$E_p = 0.2$	6	541
D. et al.	$E_p = 0.10$	2	705
TOTALS:	23	4108	

Now, to entity, however, a complication, excepting to the overall behavior of the fit, is that the lower-energy data points for the branches of the d-d reaction are not yet available at relevant to the fusion and fission of current fusion interest! The ratios of the experimental measurements<sup>13</sup> show large differences in the D(d,n) He and D(d,p) cross sections in the low-kinetic energy range. The D(d,n) differential cross section has a higher zero-to-threshold asymmetry than does the D(d,p) differential cross section, and the integrated cross section for the neutron line (files 15-17) lighter than that for the proton line (1). These differences are quite unexpected at first sight, because they occur for different reactions which one would expect to be more similar in the basis of charge symmetry. Even taking into account external charge differences in the exit-<sup>3</sup> channel (n- $^3\text{He}$  and p-T) penetrabilities, etc., would appear to give the opposite effect to that observed - i.e., the enhancement of the proton branch. However, we noticed a compensating enhancement of the neutron branch in the p-wave states coming from isospin mixing in the external Coulomb field, although it was not sufficient to explain the experimentally observed differences.

Recently, following the suggestion of Sergeev<sup>14</sup> that additional isospin mixing from the internal Coulomb interactions may reproduce the observed differences, we have allowed non-zero  $T = 1$  widths in the  $^3\text{P}_1$  states of the d-d channel (these widths are zero in the strict isospin-conservation limit). Indeed, the experimental differences are largely reproduced with mixing widths only 2% of the single-particle value which characterizes the d-d widths in the  $^3\text{P}_1$ ,  $T = 0$  levels. This is entirely consistent with the magnitude of the matrix element one might expect from internal Coulomb mixing, indicating that perhaps anomalous differences even as large as those observed in the d + d reaction cross sections may be explained entirely by Coulomb effects.

The calculations are compared to low-energy measurements of the D(d,n) and D(d,p) cross sections in Figs. 1 and 2. Figure 1 shows the isospin-mixed D(d,n) and D(d,p) integrated cross section calculations compared with various measurements at energies below 500 keV. Figure 2 shows the effect of

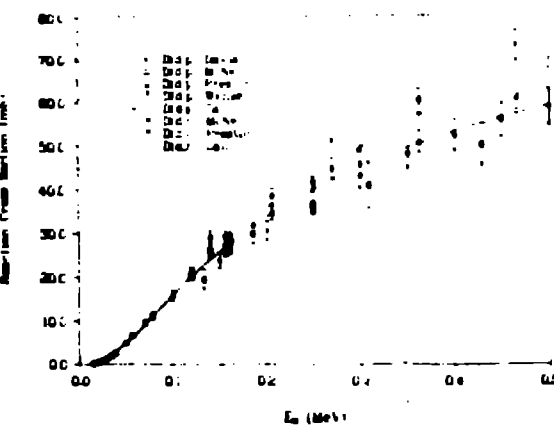


Fig. 1. R-matrix fits (solid curves) to various measurements of the D(d,n) $^3\text{He}$  (upper points) and D(d,p) (lower points) cross sections at energies below 500 keV.

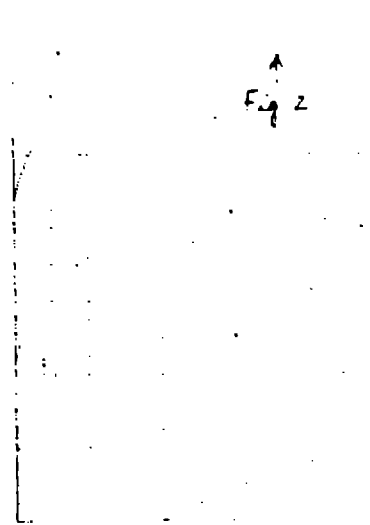


Fig. 2. Ratios of the integrated cross sections,  $C_n(0)/C_p(0)$  and  $C_n(90)/C_p(90)$ , for the two branches of the d + d reaction. The points are measurements of Theus et al.; the solid and dashed curves are R-matrix calculations with and without internal isospin mixing, respectively.

allowing internal isospin mixing in the calculations on the ratio of the integrated cross sections, and on the ratio of the differential cross section asymmetries for the two reactions. The large values of these ratios observed experimentally in the few-hundred keV region are clearly much better reproduced by including internal isospin mixing in the calculations.

The calculations including internal isospin mixing also show improved agreement with differences in the outgoing neutron and target polarizations measured at low energies. At higher energies, where differences have been seen to persist in measurements of analyzing powers for the  $d + d \rightarrow d + d$  and  $n + ^3\text{He}$  deuterons,<sup>17,18</sup> the situation is not so clear. Some of the analyses were different or are improved by the mixing, while others remain unaltered for. We plan to explore the effect of allowing internal isospin mixing in higher partial waves or these analyzing powers. In addition, we need to investigate a related consequence of internal isospin mixing that has been neglected thus far: the perturbation of the pure isospin relations between  $p + p$  and  $n + ^3\text{He}$  widths in both the  $J = 0$  and  $J = 1$  levels. However, the results of the analysis at this stage show promise for being able to account successfully for data from all the four-nucleon reactions with a single, Coulomb-corrected, charge-independent set of R-matrix parameters.

#### Five Nucleons

The discussion here will concern mainly reactions of the  $\text{He}$  cluster, which contains the most prominent of all low-energy fusion processes,  $T(d,n)^4\text{He}$ . A summary of the channels and data included in the  $^5\text{He}$  analysis is given in Table II. It can be seen that an especially large variety of data types is available for the  $T(d,n)$  reaction, including cross sections, measurements for beam and target polarized separately (analyzing power) and simultaneously (spin correlations), and measurements of outgoing neutron polarizations for both unpolarized and polarized (polarization transfer) configurations of beam and target.

Table II.  $^5\text{He}$  System Analysis

CHANNELS INCLUDED:		d-t		
		$n - ^4\text{He}$		
		$n - ^4\text{He}^*$		
Reaction	Energy Range (MeV)	No. Observ- able Types	No. Data Points	
$T(d,d)\text{T}$	$E_d = 0-8$	6	752	
$T(d,n)^4\text{He}$	$E_d = 0-8$	13	852	
$T(d,n)^4\text{He}^*$	$E_d = 4-8-8$	1	11	
$^4\text{He}(n,n)^4\text{He}$	$E_n = 0-28$	2	799	
	TOTALS:	23	2414	

The fits to a small sample of the 2400 data points are shown for the reactions  $T(d,d)\text{T}$ ,  $T(d,n)^4\text{He}$ , and

$^4\text{He}(n,n)^4\text{He}$  in Figs. 3-5. Figure 3 shows cross section and polarization angular distributions for  $T(d,d)\text{T}$  in the range  $E_d = 1.2$  to 8 MeV. Figure 4 shows fits to a selection of the  $T(d,n)^4\text{He}$  data at energies between 1 and 7 MeV; cross sections and polarizations for  $^4\text{He}(n,n)^4\text{He}$  at neutron energies between 1.6 and 24 MeV are shown in Fig. 5. These are representative of the fits to all the data included in the analysis, which are generally quite good.

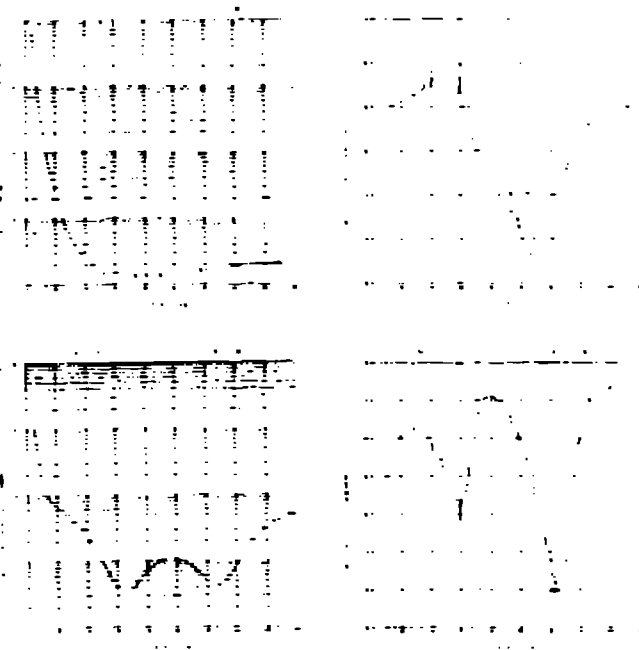
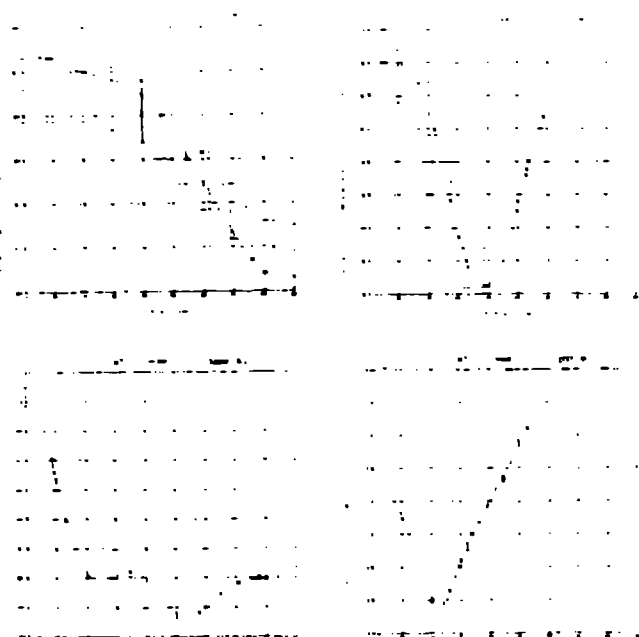


Fig. 3. Fits to  $T(d,d)\text{T}$  cross sections and analyzing powers at energies between 1.2 and 8 MeV.



Fits to  $T(d,n)^4\text{He}$  cross sections and polarization at energies between 1 and 7 MeV.

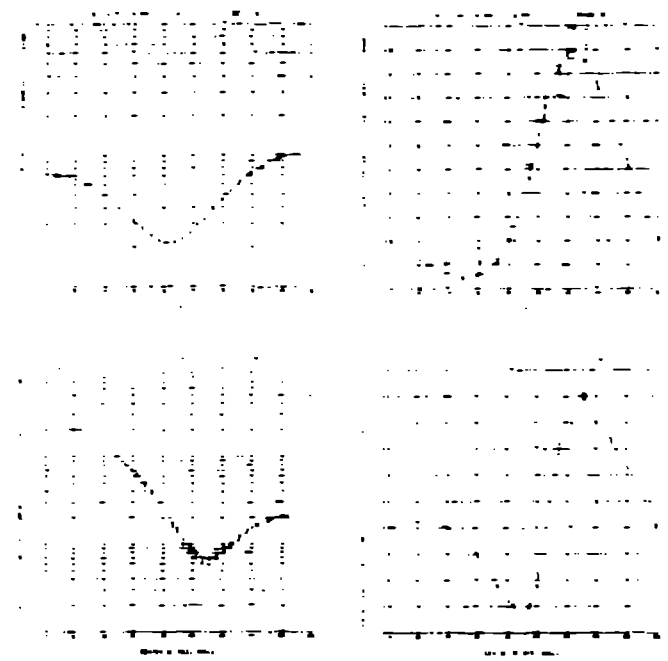


Fig. 5. Fits to  ${}^4\text{He}(n,n){}^4\text{He}$  cross sections and polarizations at energies between 0.9 and 24 MeV.

The calculated and measured observables for this system, particularly the polarizations, undergo marked changes in angular shape as a function of energy over the range of the analysis ( $E_x < 22$  MeV), due in part to the presence of ten "resonances" at excitation energies  $E_x \leq 25$  MeV in  ${}^5\text{He}$ . Only two of these produce visible structure in the integrated  $\text{T}(d,n)$  reaction cross section shown in Fig. 6. One is the famous 110-keV resonance responsible for the large low-energy cross section which makes the  $\text{T}(d,n)$  reaction such an attractive fusion energy process, and the other is a small "bump" at  $E_d = \sim 5$  MeV.

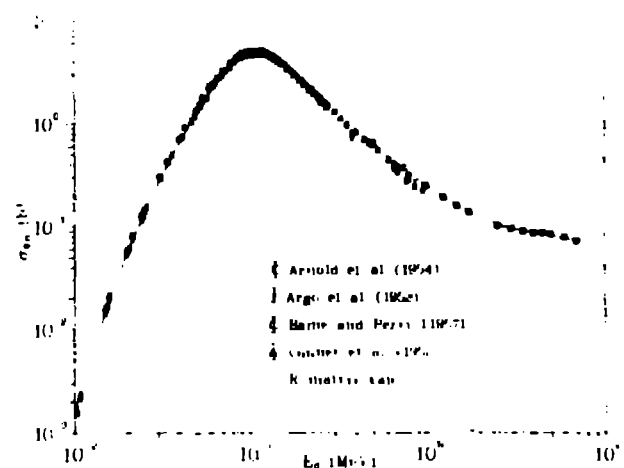


Fig. 6. R-matrix calculation (solid curve) compared to various measurements of the  $\text{T}(d,n){}^4\text{He}$  integrated cross section at energies below 8 MeV.

The effect of the 110-keV s-wave resonance on the  $\text{T}(d,n)$  cross section persists down to very low deuteron energies. This can be seen in an expanded plot of the low-energy cross sections shown in Fig. 7,

in which the inverse-energy and Gamow-penetrability dependence have been removed. What remains, the so-called "astrophysical S-function", would plot as a horizontal straight line if the assumptions implied by the usual Gamow extrapolation of the low-energy cross sections were valid. In fact, the dashed line labeled "Gamow extrapolation" corresponds to the cross section values reported by Arnold et al.<sup>17</sup> in place of their own experimental measurements<sup>18</sup> ( ) at energies below 20 keV. The R-matrix calculation clearly does not follow the Gamow dependence at low energies due to the resonance, and tends to confirm the behavior of the original measurements.<sup>18</sup>

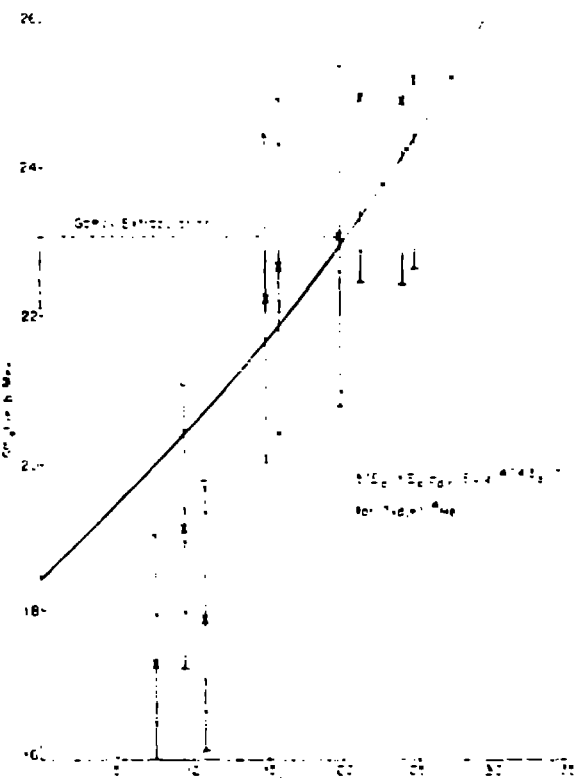


Fig. 7. Astrophysical S-function for  $\text{T}(d,n){}^4\text{He}$  as a function of laboratory energy. The solid curve is the R-matrix calculation, and the dashed line is the Gamow extrapolation reported by Arnold et al.<sup>17</sup> in place of their measured points<sup>18</sup> ( ) at energies below 20 keV.

We are also doing a similar analysis of reactions in the  ${}^3\text{Li}(\text{d},{}^3\text{He},\text{p}){}^4\text{He}$  system which uses an even more extensive data base. The calculated  ${}^3\text{He}(\text{d},\text{p}){}^4\text{He}$  integrated cross section we obtain peaks at a value nearly in the middle of the broad range of measured values that have been obtained at the peak from 100 to 900 mb. Neither of the five-nucleon analyses is yet final, since new measurements have been added recently in both cases which appear to conflict with some of the data previously being analyzed, but the essential features of the calculated reaction cross sections discussed here have not changed.

#### Six Nucleons: ${}^6\text{He}$ System

Our study of reaction in  ${}^6\text{He}$  system is motivated by large uncertainties in the  $\text{T}(\text{t},\text{n}){}^4\text{He}$  cross section

at low energies, corresponding to large discrepancies among the measurements. As can be seen in Table III, very few measurements are available for reactions in this system, making this analysis an example of one of the simplest we have yet done.

Table III.  $^6\text{He}$  System Analysis

CHANNELS INCLUDED: t-7 $n-\text{He}$ ( $2n-\text{He}$ )				
	No.	Energy Range (MeV)	Observ. Types	No. Data Points
T(t,t)T	1	$E_t=0-2$		??
T(t,2n) $^4\text{He}$	1	$E_t=0-2$		71
TOTALS:	2			96

The fits to most of the few available t-t differential elastic scattering cross section measurements are shown in Fig. 8 at triton energies between 1.6 and 2 MeV. Although these fits are quite good, it is doubtful whether they constrain very much the fit to the T(t,2n) reaction cross sections shown in Fig. 9, particularly at low energies. Nevertheless, the R-matrix calculation shows a definite preference for

the relatively recent measurements of Serov et al.<sup>19</sup> in the low-energy region. This remains the case even when the Serov data are removed from the fit, indicating that the low-energy behavior of the calculated cross section is actually being determined by consistency with the data at energies above 100 keV, where the measurements are in much better mutual agreement. Of course, the low-energy extrapolation of the cross section is to some extent a function of the extremely simple parameterization of the R-matrix necessitated by lack of data, but the agreement with the Serov data is an indication that this parameterization may be adequate at energies below 2 MeV. In particular, we take into account only contributions from the  $^6\text{He}$  ground state, and from a level which is responsible for the slight bump in the t+t reaction cross section at energies close to 2 MeV.

Large differences between our calculated curve and some of the earlier measurements at energies below 100 keV (see Fig. 9) result in significant differences between Maxwellian reaction rates calculated from the R-matrix cross sections and those based on the earlier data. Our reaction rates become a factor of two or more lower than those of Greene<sup>21</sup> and of Duane<sup>22</sup> at temperatures below  $kT = 10$  keV.

#### Seven Nucleons

Although the analysis discussed here is a charge-symmetric R-matrix analysis of all the 7-nucleon reactions, including those in both the  $^7\text{Li}$  and  $^7\text{Be}$  systems, we shall mention only the  $^7\text{Be}$  reactions. This is because similar analyses of reactions in the  $^7\text{Li}$  system have been discussed elsewhere<sup>5,6,23</sup> in connection with neutron standards applications, and because the  $^7\text{Be}$  system contains charged-particle reactions of great interest in advanced fusion concepts.<sup>2</sup>

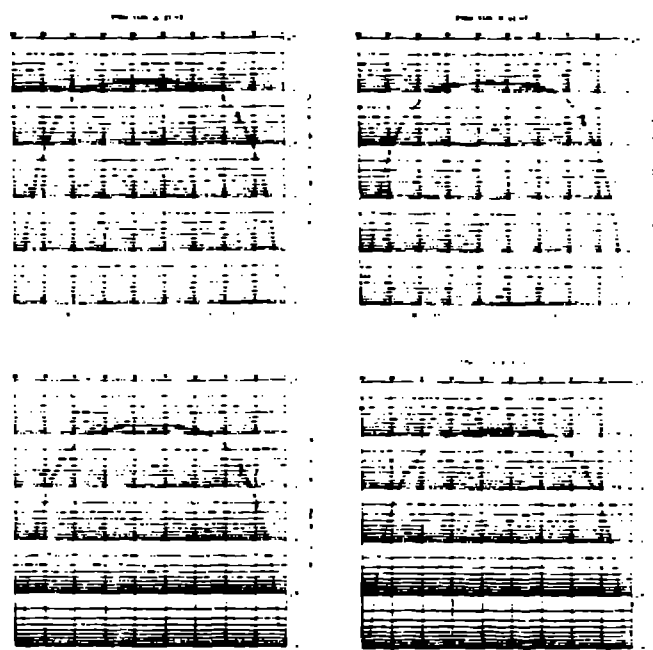


Fig. 8. Fits to T(t,t)T differential cross sections at energies between 1.6 and 2 MeV.

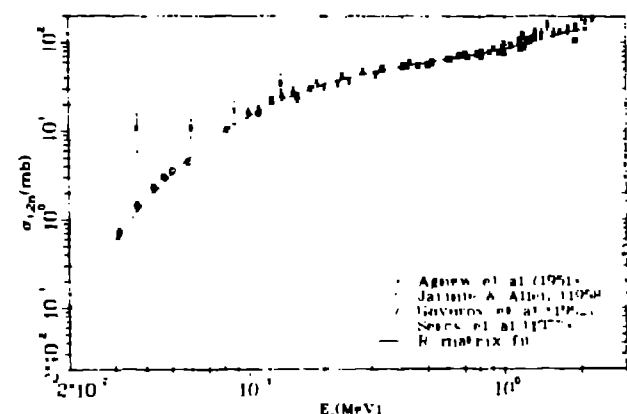


Fig. 9. R-matrix calculation (solid curve) compared with various measurements of the T(t,2n) $^4\text{He}$  integrated cross section at energies below 2 MeV.

A summary of the data included for the 7-nucleon reactions is given in Table IV. Cross section and polarization measurements are available for the four reactions possible among p- $^6\text{Li}$  and  $^3\text{He}$ - $^4\text{He}$  ( $^7\text{Be}$  system). The fits to some of these are shown for the three independent reactions  $^6\text{Li}(p,p)^6\text{Li}$ ,  $^6\text{Li}(p,\text{He})^4\text{He}$ , and  $^4\text{He}(\text{He},\text{He})^4\text{He}$  in Figs. 10-12.

The problem in the  $^6\text{Li}(p,\text{He})^4\text{He}$  reaction, which is of greatest current interest in the  $^7\text{Be}$  system, has been that the few existing differential cross section measurements have been relative, and the absolute determinations of the integrated cross section have differed by as much as 50%. In the 7-nucleon analysis we described at the Harwell conference<sup>7</sup> as an example of our charge-independent approach, the

Table IV. Seven-Nucleon Analysis

CHANNELS INCLUDED:		$p\cdot {}^6_{Li}$	$n\cdot {}^6_{Li}$
		${}^3_{He}\cdot {}^4_{He}$	$t\cdot {}^4_{He}$
<u>Reaction</u>		No. Energy Range (MeV)	Observ- able Types
${}^6_{Li}(p,p){}^6_{Li}$	$E_p = 0-2.5$	1	187
${}^6_{Li}(p, {}^3_{He}) {}^4_{He}$ -inv.	$E_p = 0-2.5$	3	559
${}^4_{He}( {}^3_{He}, {}^3_{He}) {}^4_{He}$	$E_{ {}^3_{He}} = 0-1$	2	1487
${}^6_{Li}(n,n){}^6_{Li}$	$E_n = 0-1.7$	3	330
${}^6_{Li}(n,t){}^4_{He}$	$E_n = 0-1.7$	2	468
${}^4_{He}(t,t){}^4_{He}$	$E_t = 0-11$	2	1355
TOTALS:		13	4386

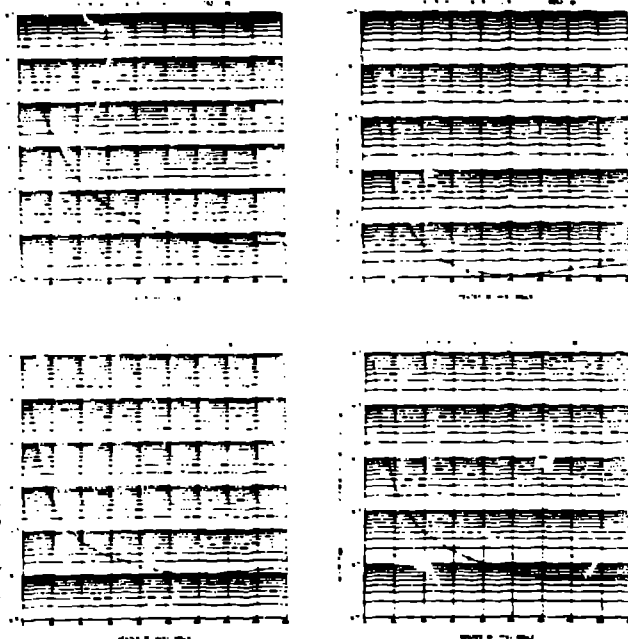


Fig. 10. Fits to  ${}^6_{Li}(p,p){}^6_{Li}$  cross sections at energies below 2.5 MeV.

experimental cross-section data included for the  ${}^6_{Li}(p, {}^3_{He}) {}^4_{He}$  reaction required extensive renormalization in almost every case. We have therefore been uncertain about the reliability of the scale of our calculated cross sections, which presumably was determined by data for other reactions in the analysis.

Recently, new absolute measurements of  ${}^6_{Li}(p, {}^3_{He}) {}^4_{He}$  differential cross sections at proton energies between 0.14 and 3 MeV have been made by Elwyn et al.<sup>22</sup> at Argonne National Laboratory. A comparison of their integrated cross sections with our predictions<sup>7</sup> is shown in Fig. 13. It can be seen that the agreement of the calculations with the new measurements is excellent, both in shape and magnitude.

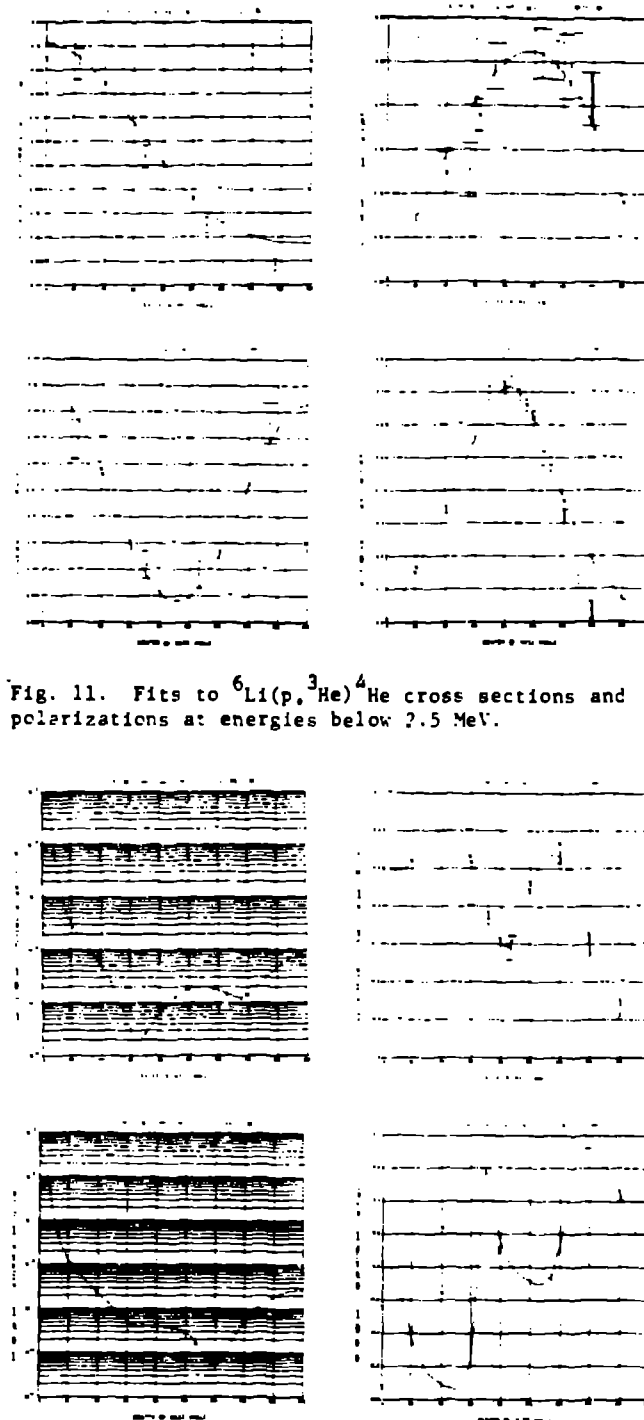


Fig. 11. Fits to  ${}^6_{Li}(p, {}^3_{He}) {}^4_{He}$  cross sections and polarizations at energies below 2.5 MeV.

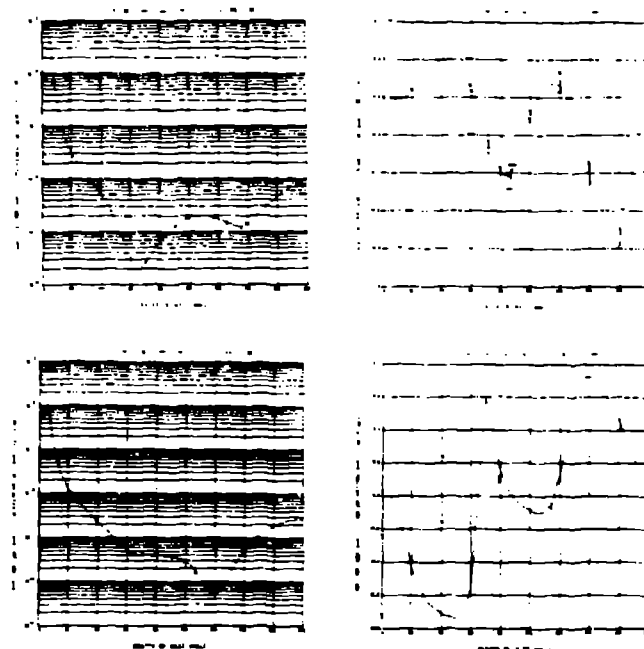


Fig. 12. Fits to  ${}^4_{He}( {}^3_{He}, {}^3_{He}) {}^4_{He}$  Cross sections and polarizations at energies below 10 MeV.

The agreement of the calculated angular distributions with the new data<sup>22</sup> is generally poorer, especially at energies above 2 MeV, indicating that somewhat different interferences among the partial-wave amplitudes are required (possibly even those involving  ${}^6_{Li}$  d-waves, which have been neglected thus far in the calculations) which do not affect the integrated cross sections.

This comparison indicates that the other 7-nucleon data in the analysis, through unitary and charge-

conjugate relationships, correctly determine the scale of the  ${}^6\text{Li}(p, {}^3\text{He})$  reaction cross section, much as other  ${}^7\text{Li}$  data had constrained values of the  ${}^6\text{Li}(n,t)$  cross section in the analysis<sup>23</sup> used for the ENDF/B-V  ${}^6\text{Li}$  evaluation at low energies.

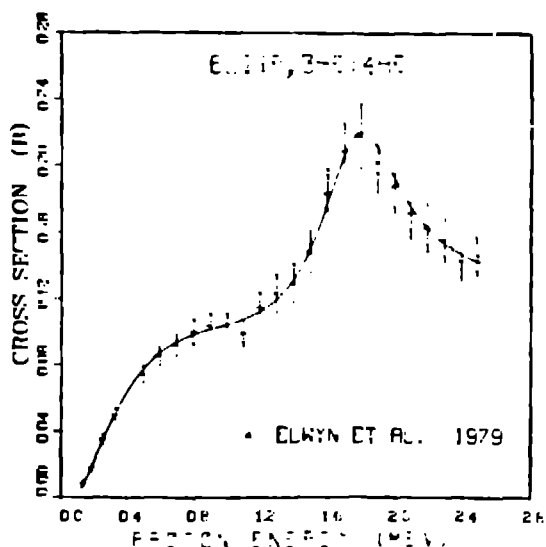


Fig. 13. Predictions from the charge-symmetric 7-nucleon analysis<sup>7</sup> compared with recent measurements of Elwyn et al.<sup>22</sup> for the  ${}^6\text{Li}(p, {}^3\text{He}){}^4\text{He}$  integrated cross section.

#### Conclusions

As the examples described in the previous section suggest, a great deal of information is available from these multireaction R-matrix analyses, having been determined in most cases by a large and varied collection of experimental input. Clearly, the R-matrix parameters provide detailed information about the spectroscopy of light systems, and even information about the macroscopic properties of nuclear forces. Of more direct concern to the subject of this conference, however, are the smooth (as functions of both energy and angle) charged-particle cross sections which result from them.

The dominance of Coulomb effects in charged-particle cross sections at low energies is modified by nuclear resonances in many cases of interest in fusion applications. This is most apparent for the T(d,n) reaction, but is true to some degree for all the reactions discussed. R-matrix theory provides a framework for fitting and extrapolating these cross sections in which both the long-range effects, like penetration of the Coulomb-angular momentum barrier, and the short-range (nuclear) effects arise in a simple and physically meaningful way. Moreover, the interaction of these effects in the theory leads in general to a different energy dependence for the low-energy cross sections than that obtained from the representations of fusion cross sections commonly

used.<sup>24</sup> There are indications from the T(d,n) and T(t,2n) examples that the R-matrix dependence is more nearly correct, but a firm conclusion requires more and better-quality measurements in the low-energy region, such as those forthcoming from the fusion cross-section measurement program at Los Alamos.<sup>3</sup>

At higher energies, the reactions appear to be dominated by broad, overlapping structures, few of which appear as definite bumps in the integrated cross sections. These structures can be associated with definite R-matrix levels, however, with the help of angular distribution measurements, particularly those for polarization observables. Attempting to use all the available experimental data in these analyses also has obvious statistical advantages, especially in cases where direct measurements of the cross sections are conflicting or incomplete. In those cases, the other data included, even for different reactions, can help dictate more correct values for cross sections, as illustrated by the p+ ${}^6\text{Li}$  example.

We feel that such R-matrix analyses, making maximal use of the available experimental data while imposing some minimal information about nuclear forces, constitute the best technique currently at hand for evaluating light-element cross sections. One obtains from these analyses unified cross-section sets, in which the elastic scattering and reaction cross section for a given system are calculated from the same R-matrix parameters. We therefore suggest that compilers of evaluated charged-particle cross sections make use of these calculations, where available, rather than rely on methods having less physical content and experimental input.

#### Acknowledgments

K. Witte, who developed and maintains the EDNA code, has been our collaborator on several of these analyses. Likewise, S. D. Baker and E. K. Bieger collaborated with us on analyses of the 7-nucleon reactions.

#### References

1. C. E. Beall, "Nuclear Data Requirements of the U.S. - West Fusion Power Program of the United States of America," presented at IAEA Advisory Group Meeting on Nuclear Data for Fusion Reactor Technology, Vienna, Austria (1978).
2. R. W. Conn, Bull. Am. Phys. Soc., 20, 561 (1975).
3. N. Jarmie, Bull. Am. Phys. Soc., 20, 849 (1975).
4. D. C. Dodder et al., "Models Based on Multichannel R-Matrix Theory," JAERI-M 5984, p. 1 (1975).
5. G. M. Hale, "R-Matrix Analysis of the Light Element Standards," NBS Spec. Publ. Publication 425, p. 302 (1975).
6. G. M. Hale, "R-Matrix Methods for Light Systems," IAEA-90, Vol. II, p. 1 (1976).
7. D. C. Dodder and G. M. Hale, "Applications of Approximate Isospin Conservation in R-Matrix Analyses," in Neutron Physics and Nuclear Data (Harwell), p. 490 (1978).
8. A. M. Lane and D. Robson, Phys. Rev., 151, 774 (1966).
9. E. P. Wigner and L. Eisenbud, Phys. Rev., 72, 279 (1947).
10. A. M. Lane and R. G. Thomas, Rev. Mod. Phys., 30, 257 (1958).
11. D. C. Dodder, K. Witte, and G. M. Hale, "EDNA, an Energy Dependent Analysis Code for Nuclear Reactions," (unpublished).

conjugate relationship: correctly determine the scale of the  ${}^6\text{Li}(p, {}^3\text{He})$  reaction cross section, much as other  ${}^7\text{Li}$  data had constrained values of the  ${}^6\text{Li}(n,t)$  cross section in the analysis<sup>23</sup> used for the ENDF/B-V  ${}^6\text{Li}$  evaluation at low energies.

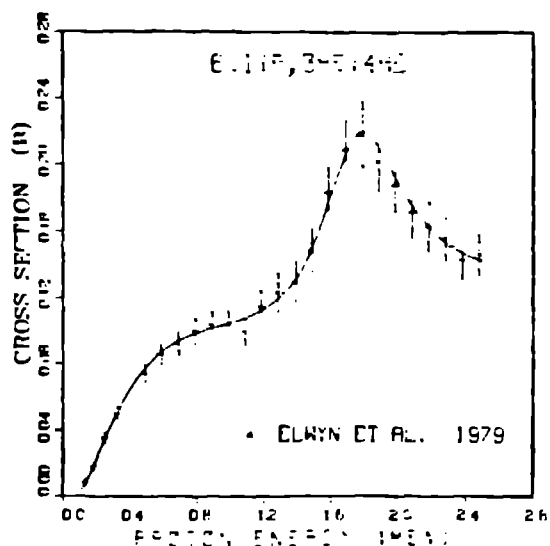


Fig. 13. Predictions from the charge-symmetric 7-nucleon analysis<sup>7</sup> compared with recent measurements of Elwyn et al.<sup>22</sup> for the  ${}^6\text{Li}(p, {}^3\text{He}){}^4\text{He}$  integrated cross section.

#### Conclusions

As the examples described in the previous section suggest, a great deal of information is available from these multireaction R-matrix analyses, having been determined in most cases by a large and varied collection of experimental input. Clearly, the R-matrix parameters provide detailed information about the spectroscopy of light systems, and even information about the macroscopic properties of nuclear forces. Of more direct concern to the subject of this conference, however, are the smooth (as functions of both energy and angle) charged-particle cross sections which result from them.

The dominant effect of Coulomb effects in charged-particle cross sections at low energies is modified by nuclear resonances in many cases of interest in fusion applications. This is most apparent for the  $T(d,n)$  reaction, but is true to some degree for all the reactions discussed. R-matrix theory provides a framework for fitting and extrapolating these cross sections in which both the long-range effects, like penetration of the Coulomb-angular momentum barrier, and the short-range (nuclear) effects arise in a simple and physically meaningful way. Moreover, the interaction of these effects in the theory leads in general to a different energy dependence for the low-energy cross sections than that obtained from the representations of fusion cross sections commonly

used.<sup>24</sup> There are indications from the  $T(d,n)$  and  $T(t,2n)$  examples that the R-matrix dependence is more nearly correct, but a firm conclusion requires more and better-quality measurements in the low-energy region, such as those forthcoming from the fusion cross-section measurement program at Los Alamos.<sup>3</sup>

At higher energies, the reactions appear to be dominated by broad, overlapping structures,  $f_0$  of which appear as definite bumps in the integrated cross sections. These structures can be associated with definite R-matrix levels, however, with the help of angular distribution measurements, particularly those for polarization observables. Attempting to use all the available experimental data in these analyses also has obvious statistical advantages, especially in cases where direct measurements of the cross sections are conflicting or incomplete. In those cases, the other data included, even for different reactions, can help dictate more correct values for cross sections, as illustrated by the  $p+{}^6\text{Li}$  example.

We feel that such R-matrix analyses, making maximal use of the available experimental data while imposing some minimal information about nuclear forces, constitute the best technique currently available for evaluating light-element cross sections. One obtains from these analyses unified cross-section sets, in which the elastic scattering and reaction cross section for a given system are calculated from the same R-matrix parameters. We therefore suggest that compilers of evaluated charged-particle cross sections make use of these calculations, where available, rather than rely on methods having less physical content and experimental input.

#### Acknowledgments

K. Witte, who developed and maintains the EDA code, has been our collaborator on several of these analyses. Likewise, S. D. Baker and E. K. Bieger collaborated with us on analyses of the 7-nucleon reactions.

#### References

1. T. R. Cook, "Nuclear Data Requirements of the Magnetic Fusion Power Program of the United States of America," presented at IAEA Adris meeting on Meeting on Nuclear Data for Fusion Power Technology, Vienna, Austria (1978).
2. R. W. Conn, Bull. Am. Phys. Soc. 24, 861 (1979).
3. N. Jarmic, Bull. Am. Phys. Soc. 24, 863 (1979).
4. D. C. Dodder et al., "Models Based on Multichannel R-Matrix Theory," JAERI-M 5984, p. 1 (1975).
5. G. M. Hale, "R-Matrix Analysis of the Light Element Standards," NBS Special Publication 425, p. 302 (1975).
6. G. M. Hale, "R-Matrix Methods for Light Systems," IAEA-90, Vol. II, p. 1 (1976).
7. D. C. Dodder and G. M. Hale, "Applications of Approximate Isospin Conservation in R-Matrix Analyses," in Nearron Physics and Nuclear Data (Harwell), p. 490 (1978).
8. A. M. Lane and D. Robson, Phys. Rev. 151, 77 (1966).
9. F. P. Wigner and L. Eisenbud, Phys. Rev. 72, 24 (1947).
10. A. M. Lane and R. G. Thomas, Rev. Mod. Phys. 30, 257 (1958).
11. D. C. Dodder, K. Witte, and G. M. Hale, "EDA, an Energy Dependent Analysis Code for Nuclear Reactions," (unpublished).

12. G. M. Hale, J. Devaney, D. C. Dodder, and K. Witte, Bull. Am. Phys. Soc. 19, 506 (1974).
13. See, for instance, R. B. Theus, W. J. McGary, and L. A. Beach, Nucl. Phys. 80, 273 (1966).
14. V. A. Serpeyev, Phys. Lett. 38B, 246 (1971).
15. V. Ezhin et al., "Investigation of Charge-Symmetry Violation in the Mirror Reactions  $^2\text{H}(d, p)^3\text{H}$  and  $^3\text{He}(d, p)^4\text{He}$ ," submitted to Nucl. Phys. (1979).
16. T. R. Duncanson, Ohio State University, personal communication (1979).
17. V. K. Arnold et al., Phys. Rev. 93, 463 (1954).
18. V. K. Arnold et al., "Absolute Cross Section for the Reaction  $^7\text{Li}(d, n)^6\text{Li}$  from 10 to 120 keV," LA-1074 (1953).
19. V. I. Serov, S. N. Abramovich, and L. A. Merkin, At. Energ. 39, 7 (1975).
20. S. L. Greene, "Maxwell-Averaged Cross Sections for Some Thermonuclear Reactions on Light Isotopes," UCRL-70527 (1967).
21. B. H. Dancock, "Fusion Cross Section Theory," BNWL-1695, p. 75 (1972).
22. A. J. Flawn et al., "Cross Sections for the  $^6\text{Li} + ^3\text{He}$  Reaction at Incident Energies 1.1 and 1.7 MeV," submitted to Phys. Rev. C (1979).
23. G. M. Hale, "R-Matrix Analysis of the  $^7\text{Li}$  System," NBS Special Publication 442, p. 100 (1977).
24. In these representations, Coulomb effects are not explicit in the  $t$ -functions. The simplest example is the Gamow energy integral in constant  $t$ . For example, see Ref. 21, Ref. 22, and A. Ieraso, *J. Appl. Phys.*, 55, 1764 (1984).